Antimalarial Drug Discovery: Structural Insights

Lunev, Sergey

Chapter 7

Purification, crystallization and preliminary X-ray diffraction analysis of pyridoxal kinase from *Plasmodium falciparum* (*Pf*PdxK)

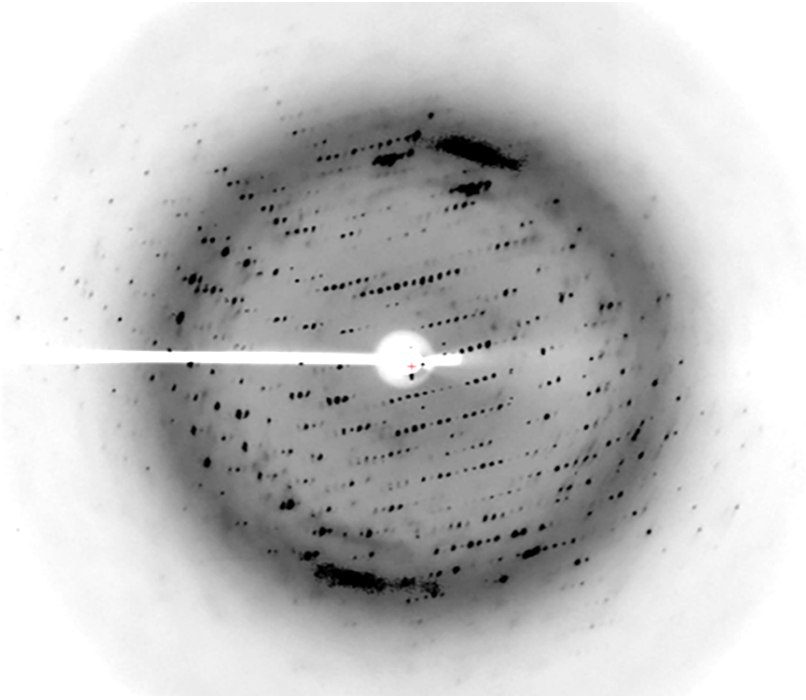

This chapter has been published
Thales Kronenberger*, **Sergey Lunev***, Carsten Wrenger & Matthew R. Groves.
Acta Crystallogr F Struct Biol Commun. 2014;70:1550-5.
*Authors contributed equally

Abstract

Pyridoxal kinases (PdxK) catalyze the phosphorylation of vitamin B6 precursors. Thus, these enzymes are an essential part of many metabolic processes in all organisms. The protozoan parasite *Plasmodium falciparum* (the main causative agent of Malaria tropica) possesses a unique *de novo* B6-biosynthesis pathway in addition to an interconversion pathway based on the activity of plasmodial PdxK (*Pf*PdxK). The role of PdxK in B6 salvage has prompted previous authors to suggest PdxK as a promising target for structure-based antimalarial drug design. Here, the expression, purification, crystallization and preliminary X-ray diffraction analysis of *Pf*PdxK are reported. *Pf*PdxK crystals have been grown in space group P21, with unit-cell parameters a = 52.7, b = 62.0, c = 93.7 A°, α = 90°, β = 95°, γ = 90°. A data set has been collected to 2 A° resolution and an initial molecular replacement solution is described.

1. Introduction

Malaria remains a major health problem, as approximately half of the world's population lives in regions where it is transmitted (*i.e.*, in most parts of the tropics and subtropics). Malaria is caused by infection with one of several species of the genus *Plasmodium*, of which *Plasmodium falciparum* is responsible for the most severe and lethal form [1]. In 2012, *Plasmodium* infected over 200 million and killed at least 600,000 people worldwide [2]. The actual number of deaths and infections is likely to be higher, as in many cases the data is unavailable or undocumented. There is as yet no effective vaccine available against malaria and the parasite rapidly develops resistance to drugs used for its treatment, making the identification of new drug targets important for global health [3-5]. New antimalarial agents that provide higher efficacy and less toxicity are urgently required.

A member of the ribokinase superfamily, pyridoxal kinase (PdxK) functions in the vitamin B_6 salvage pathway [6] and catalyzes the phosphorylation of pyridoxal, pyridoxine and pyridoxamine into precursors of the active form of B_6 (PLP) [7]. This active form is essential for both prokaryotes and eukaryotes as it is involved in a variety of metabolic processes as a cofactor, as well as in combating oxidative stress caused by singlet oxygen [8, 9]. For example PLP is an essential cofactor in the activity of plasmodial Aspartate aminotransferase (*Pf*AspAT), which has been suggested to be a drug target as it bridges both carbon metabolism and nucleotide biosynthesis [10-12]. Unlike mammalian cells, *P. falciparum* has a functional pathway for B_6 *de novo* biosynthesis [13], which has already been validated as a drug-target [14]. Additionally the parasite possesses an interconversion pathway based on PdxK, which has already been exploited for pro-drug discovery [15].

Pyridoxal kinases have been structurally characterized in several organisms including *H. sapiens* [16], *E. coli* [17], *B. subtilis* [18], *A. thaliana* [19] and in the parasite *T. brucei* [20]. PdxK has been proven to be essential for growth of *T. brucei*, as knock-out parasites were unable to survive in PLP-free medium [21].

The availability of a crystal structure of the plasmodial PdxK (*Pf*PdxK)

is essential in the dissection of the unique vitamin B_6 salvage pathway of *P. falciparum* [13] and its validation as a drug target in the treatment of malaria. It will provide new details into the mechanism of the B_6 interconversion pathway and can also be used in comparative studies with PdxK homologs from other organisms. *Pf*PdxK is a polypeptide of 497 amino acids with a predicted molecular mass of 57.2kDa [13]. Sequence analysis of wild-type *Pf*PdxK shows that it contains a 205-amino-acid insert (109–314) that has no structural homologues. The 292 amino acids N- and C-terminal to this insert (51% of the sequence) can be aligned with the *H. sapiens* PdxK (GenBank accession O00764) with 32% identity, resulting in an overall identity of 16%. The structural and functional differences could be used in the design of selective antimalarials.
Here we report the expression, purification, crystallization and preliminary X-ray diffraction characterization of *Pf*PdxK.

2. Methods

2.1. Macromolecule production

2.1.1. Cloning of *Pf*PdxK

The PdxK gene of *P. falciparum* was amplified by polymerase chain reaction (PCR) using *P. falciparum* 3D7 cDNA as template and sequence-specific sense (5'-GCGCCCGCGGTATGAAGAAGGAAAATATTATCTCC -3') and antisense (5'- GCGCCCATGGGCAAAAAAAACAGGCTCTTC-3') oligonucleotides containing *Ac*II and *Nco*I restriction sites, respectively (Table 1). The PCR was performed with *Pfu* polymerase using the following conditions: one cycle of 367K for 7 min followed by 35 cycles of 1 min at 367K, 1.5 min at 315K and 2 min at 341K, according to [13]. The PCR fragments were cloned into pASK-IBA3 previously digested with *Bsa*I and the nucleotide sequence was determined by automated sequencing (Seqlab, Germany). Nucleotide-sequence and protein-sequence analyses were performed using the software Gene Runner. The final construct consisted of full-length *Pf*PdxK with the additional amino acids GHHHHHH (6 His-tag) at the N-terminus (Table 1).

2.1.2. Expression of *Pf*PdxK

*Pf*PdxK was recombinantly expressed in *Escherichia coli* Rosetta 2 (DE3) (Novagen) using the expression plasmid pASK-IBA3-*Pf*PdxK, which contains the open reading frame for the *Pf*PdxK gene fused to a N-terminal His-tag to facilitate purification. Recombinant protein was purified *via* nickel-chelating chromatography employing the N-terminal His tag according to the manufacturer's recommendations (Macherey and Nagel, Germany). Transformed *E. coli* Rosetta 2 (DE3) cells were propagated in 2L of selective media (LB in the presence of 50 µg mL^{-1} Ampicillin, 35 µg mL^{-1} Chloramphenicol, 4 mM $MgCl_2$) at 310K in 2L baffled Erlenmeyer flasks (Nalgene) and induced at an OD_{600} of 0.6 with 200 ng mL^{-1} anhydrotetracycline (AHT). After induction, the temperature of the culture was lowered to 291K and the cells were incubated over night. Subsequently, they were harvested by centrifugation at 10,000 x *g* for 30 min.

2.1.3. Purification of *Pf*PdxK

The bacteria pellet was resuspended in 30 mL Lysis buffer *A* [100 mM Tris pH 8.0, 300 mM NaCl, 20 mM imidazole, 5% (v/v) glycerol and 0.1 mM β-mercaptoethanol (BME)]. The cells were lysed on ice by sonication and the homogenate was clarified by centrifugation at 45'000 x *g* for 60 min. It was not necessary to supplement the lysis buffer with lysozyme as sonication was sufficiently effective.

The supernatant containing the soluble His-tagged protein was filtered using a 0.45 µm filter (Whatman) and incubated for 10 min with 1.0 ml Ni-NTA affinity resin (Ni-NTA Agarose, Protino, Macherey Nagel, Germany) at room temperature. Recombinant protein was purified employing the C-terminal His-tag according to the manufacturer's recommendations. The following steps were also performed at room temperature as no significant protein degradation was observed. The resin was poured into a gravity-flow column (Bio-Rad) and washed with 50 mL lysis buffer (as defined above), followed by 10 mL wash buffer [100 mM Tris pH 8.0, 300 mM NaCl, 50 mM imidazole, 5% (v/v) glycerol, 3 mM BME]. The protein was eluted with elution buffer [50 mM Tris pH 8.0, 250 mM NaCl,

0.3 M imidazole, 5% (v/v) glycerol, 3 mM BME].
The eluate was collected and concentrated to a volume of 1 mL and applied onto a HiLoad 16/60 Superdex 75 column (GE Healthcare) previously equilibrated with 10 mM 2-(N-morpholino)ethanesulfonic acid (MES) pH 6.5, 100 mM NaCl, 100 mM ammonium nitrate, 5% v/v glycerol, 2mM BME. The gel-filtration buffer was chosen based upon a Thermofluor-based stability assay [22, 23](Figure 1), as previous crystallization attempts resulted in crystals unsuitable for diffraction experiments. Thermofluor data were collected on a CFX96 Real-Time System (Bio-Rad). SYPRO Orange (Invitrogen) was added to the protein sample (concentrated to 2 mg mL^{-1}) at 1:500 dilution. Experiments were composed of 45 µL of the buffer component to be screened and the 5 µL of the protein/dye solution. Inflection points in graphs of relative fluorescence units (RFU) against temperature were determined manually and used as an indicator of the sample thermal stability in the buffer component screened. Comparisons were made against a control sample containing only water. The final purified protein eluted as a single peak. This peak was pooled and concentrated using a Spin-X UF concentration unit with a 10 kDa cut-off (Corning). The final protein concentration was determined to be 10 mg mL^{-1} based upon its theoretical absorbance at 280 nm [$Abs_{0.1\%}$(1 mg ml^{-1}) = 0.49; http://web.expasy.org/protparam/]. The protein was immediately used in crystallization trials. The protein purity was estimated to be better than 95% (Figure 1a) as assessed by Coomassie Brilliant Blue-stained SDS-PAGE [24]. The final yield of purified *Pf*PdxK was approximately 5 mg per litre of culture.

2.2. Crystallization of *Pf*PdxK

Concentrated protein was submitted to the EMBL Hamburg high-throughput crystallization facility [25] for initial screening against the Classics and Classics II Suites (Qiagen) sparse-matrix screening kits. All crystallization was performed at 293 K using equal volumes (200 nL) of protein solution and crystallization reagent. Small crystals were observed in multiple conditions. Manual hanging-drop optimization screens were performed around these conditions in order to reproduce and improve the crystal size

by varying the precipitant concentration, buffer and pH. Optimised trials were performed using the hanging drop method, in which 1 μL of protein solution at a concentration of 10 mg mL^{-1} was mixed with an equal amount of reservoir solution and equilibrated over 1 mL of the reservoir solution at 293 K. Diffraction quality crystals were obtained in 0.1 M HEPES pH 7.75, 0.2 M $CaCl_2$, 31% (v/v) PEG 400, 5% (v/v) glycerol (Table 2, Figure 2a). Crystals appeared after 24 h and were suitable for diffraction studies after one week.

2.3 Data collection and processing

2.3.1. Diffraction analysis

*Pf*PdxK crystals were directly flash-cooled to 100K in the nitrogen stream at the beamline. After initial analysis using the software BEST [26, 27] a 2.0-Å dataset was collected at X12 beamline (EMBL, DESY, Hamburg) using a beam size of 200 x 200 μm. Data-collection parameters are indicated in Table 3. The space group of the *Pf*PdxK crystals was determined to be $P2_1$, with cell parameters of a=52.7, b=62.0, c=93,7, α=90°, β=95°, γ=90°. Based on these cell parameters, a single *Pf*PdxK molecule is expected in the asymmetric unit with a Matthews' coefficient of 2.87 $Å^3$ Da^{-1} and a solvent content of 57% [28]. Data were reduced using the XDS/SCALE [29, 30]. Data were merged using AIMLESS. An R_{free} set [31] for use in subsequent structure refinement and validation was created using 5% of the reflections selected at random. The data set was examined for indications of twining, but no statistically significant twining could be found.

2.3.2 Molecular Replacement

Molecular replacement was performed using the BALBES pipeline [32]. Automated database searching within *BALBES* provided a number of homologous structures for use as molecular-replacement models. An initial solution was found using the coordinates of sheep brain PdxK (PDB entry 1RFU, [33]) as a search model. This solution was found using the 1RFU structure sequence modified for molecular replacement to match the se

Table 1.

Source organism	*P. falciparum*
DNA source	*P. falciparum* 3D7 cDNA
PlasmoDB ID	PF3D7_0616000
Forward primer	5–GCGCCCGCGGTATGAAGAAGGAAAATATTATCTCC–3
Reverse primer	5–GCGCAAGCTTCTA*ATGATGATGATGATGATG*TCCAAAAAAA ACAGGCTCTTCTTTAATTAAAATATC–3
Expression vector	pASK-IBA3 (IBA Lifesciences)
Expression host	*E. coli* Rosetta 2 (DE3)
Complete amino-acid sequence of the construct produced	*MGDRG*MKKENIISIQSQVFDGFCGNNIAAFVFRRRGHIPKILNTVQY YSKFKHSGVELNSQEVDIILSEYNKDQEFMNDSNIYFLTGYIKNAEC VDMVTKNILELRRKRKIHRGKSNDNNMNGHMNGHMNGHMNGHMNGHM NGHMNGHMNGHMNGHMNGHMNGHTNGHMNGHMNDHMNGHMNGH TNDHMNGHTNDHMNGHTNDHMNGHTNDHMNDHMNGHTNDHMNDHMND HMNGHTNSHTHGLTNGHMDEPNGEHPYRLMNSNELKSSHQIIPQGKQ IHEKDMLKNNILTISQGRKKDEELYFIENIINLNFLWVCDPVMGDNG RLYVDERVVESYKKAIEYVDIITPNQYETELLCGIKINEEKDVIKCL DVLLHKGVKIVIITSVNYNFDKDHLFLYVSFFNNKNKIVYFKYKILK IHFNCFGSGDLFSCLLSFIVKQKGNILHIISKVLNIVQNVIKNSLTG LELNIIENQDIIASDGLINDILIKEEPVFF*GHHHHHH*
Length of the construct (amino acids)	508
Molecular weight of the construct (kDa)	58.5
Abs 0.1% (1mg ml^{-1}) of the construct	0.48
Complete amino-acid sequence of wild-type *Pf*PdxK	MKKENIISIQSQVFDGFCGNNIAAFVFRRRGHIPKILNTVQYYSK– FKHSGVELNSQEVDIILSEYNKDQEFMNDSNIYFLTGYIKNAECVD– MVTKNILELRRKRKIHRGKSNDNGNMNGHMNGHMNGHMNGHMNGHMN GHMNGHMNGHMNGHMNGHMNGHMNGHTNGHMNGHMNDHMNGHMNG– HTNDHMNGHTNDHMNGHTNDHMNGHTNDHMNDHMNGHT– NDHMNDHMNDHMNGHTNSHTHGLTNGHMDEPNGEHPYRLMN– SNELKSSHQIIPQGKQIHEKDMLKNNILTISQGRKKDEELY– FIENIINLNFLWVCDPVMGDNGRLYVDERVVESYKKAIEYVDIIT– PNQYETELLCGIKINEEKDVIKCLDVLLHKGVKIVIITSVNYNFD– KDHLFLYVSFFNNKNKIVYFKYKILKIHFNCFGSGDLFSCLLLS– FIVKQKGNILHIISKVLNIVQNVIKNSLTGLELNIIENQDIIASDG– LINDILIKEEPVFF
Length of the wild-type *Pf*PdxK (amino acids)	497

Molecular weight of wild-type *Pf*PdxK (kDa)	57.2
Abs0.1% (1mgml1) of wild-type *Pf*PdxK	0.49

Macromolecule-production information. The *Sac*II (forward primer) and *Hin*dIII (reverse primer) cleavage sites are underlined and the six-His tag is underlined and shown in italics both in the reverse primer and in the complete construct sequence.

quence of *Pf*PdxK, with a Z-score of 4.6 and *R* and R_{free} factors of 0.546 and 0.546, respectively. Amino acids of the search model (PDB entry 1RFU) that were identical to the *Pf*PdxK sequence were left unmodified, while non-identical amino acids were truncated to the last common atom, with the chemical identity of the atom changed to match the *Pf*PdxK sequence when necessary. Initial restrained refinement was performed within the *BALBES* automated pipeline, using REFMAC5 [34]. This resulted in a model containing the aligned portions of *Pf*PdxK (amino acids 5-103 and 310-485), with *R* and R_{free} factors of 0.482 and 0.506, respectively (Figure 3a,b; Table 3).

Table 2.

Method	Hanging drop
Temperature (K)	293
Protein concentration (mgml1)	10
Buffer composition of protein solution	10 mM MES pH 6.5, 0.1 M NaCl, 0.1 M ammonium nitrate, 5% (v/v) glycerol, 2 mM BME
Composition of reservoir solution	0.1 M HEPES pH 7.75, 0.2 M CaCl2, 31% (v/v) PEG 400, 5% (v/v) glycerol
Volume and ratio of drop (nl)	200, 1:1
Volume of reservoir (ml)	1
Crystal size (maximal dimension) (m)	100

Crystallization parameters

Figure 1

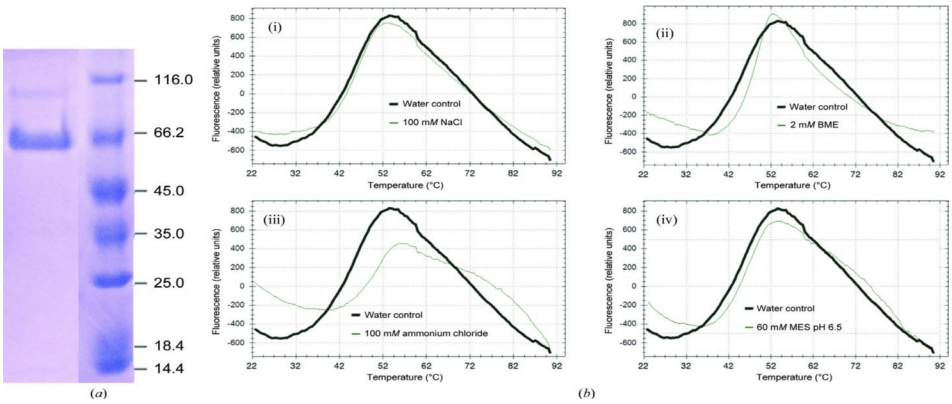

Figure 1. (a) 8% SDS–PAGE of the purified *Pf*PdxK. Sample was boiled in SDS-loading buffer prior to loading and the gel was stained with Coomassie Blue. Left lane, *Pf*PdxK sample. Right lane, unstained protein marker (Thermo Scientific; labelled in kDa). (b) Thermal shift assay results for *Pf*PdxK. When exposed to sodium chloride (i), BME (ii), ammonium chloride (iii) and MES pH 6.5 (iv) *Pf*PdxK samples showed positive shift in thermal stability.

Figure 2.

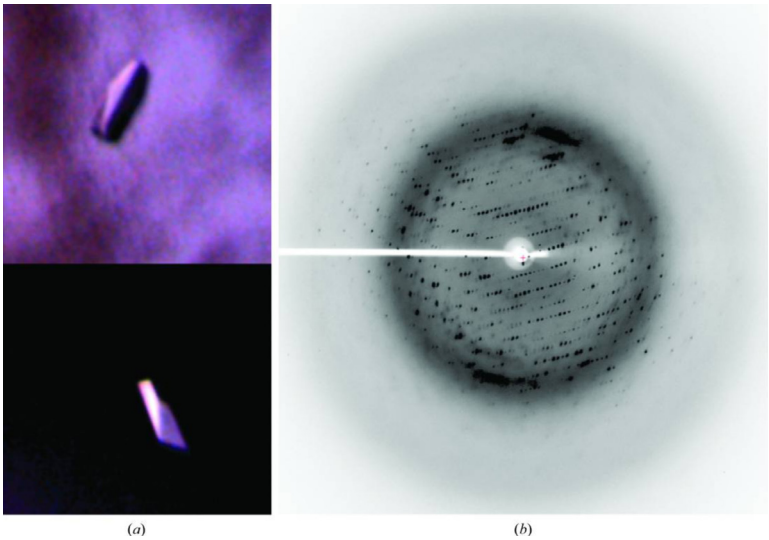

Figure 2. (a) Diffraction-quality single *Pf*PdxK crystals grown in 0.1 M HEPES pH 7.75, 0.2 M CaCl2, 31% (v/v) PEG 400, 5% (v/v) glycerol. (b) Example of the diffraction frame obtained from a *Pf*PdxK crystal on beamline X12 at the EMBL, Hamburg. The edge of the detector corresponds to a resolution of 2 Å. The corresponding beamline parameters are given in Table 3

3. Results and Discussion

We have reported the availability of *Pf*PdxK crystals suitable for diffraction analysis. The initial crystallization conditions for *Pf*PdxK were obtained using the EMBL high-throughput crystallization facility [25] and subsequently refined using manual hanging drop screens. Small crystals (5–10 *μm) were obtained when Pf*PdxK was concentrated in a buffer composed of 10 mM Tris pH 8.0, 150 mM NaCl prior to crystallization screening. However, the small crystal size resulted in poor diffraction (8–10 *Å resolution) unsuitable for structure determination*.

Table 3

Data-collection statistics:	
Beamline	X12, EMBL Hamburg
Wavelength (Å)	1 Å (12.398 keV)
Temperature (K)	100, Oxford Cryostream 700 series
Oscillation range (°)	0.2
Detector	MARCCD 245
Crystal-to-detector distance (mm)	180
No. of frames	600
Exposure per frame (s)	36
Data-integration statistics:	
Space group	P 2_1
Unit cell parameters	a=52.7, b=62.0, c=93.7 α=90°, β=95°, γ=90°
Resolution limits (Å)	8.92 – 1.99 (2.05-1.99)
Total No. of reflections	39368 (2753)
Multiplicity	2.55 (2.50)
Completeness (%)	95.3 (90.1)
R_{merge} (%)	4.4 (78.8)
Mean I/σ(I)	13.11 (1.35)

Results of data collection from *Pf*PdxK crystals

R_{merge} is defined as $\Sigma_{hkl}\Sigma_i|I_i(hkl)-<I(hkl)>|/\Sigma_{hkl}\Sigma_i I_i(hkl)$, where $I_i(hkl)$ is the *i*th intensity measurement of reflection *hkl* and $<I(hkl)>$ is the average intensity from multiple observations.

An important step was the optimization of the gel-filtration buffer using the Thermofluor method [22, 23]. As shown in Fig. 1 (b), *Pf*PdxK shows increased thermal stability in the presence of β-mercaptoethanol (+5 K), ammonium chloride (+7 K) and MES pH 6.5 (+2 K) with respect to a water control. Thermofluor analysis also indicated that 100 mM NaCl was the optimal ionic strength of NaCl, with higher concentration of NaCl resulting in thermal destabilization. Optimized *Pf*PdxK crystals suitable for diffraction measurements were obtained from the protein concentrated to 10 mg mL^{-1} in gel-filtration buffer in a 1:1 ratio with 0.1 M HEPES pH 7.75, 0.2 M $CaCl_2$, 31% (v/v) PEG 400, 5% (v/v) glycerol. The optimized crystals used for data collection had maximal dimensions of 100 μm and diffracted to 2 *Å resolution on beamline X12 at EMBL (Hamburg). The data collection and processing statistics are shown in table* 3. While the data quality in the highest resolution bin is relatively poor (R_{merge} = 51.7 %), sufficient signal exists for the use of this data in refinement based on maximum likelihood algorithms (I/s(I) = 2.03, [34]). An example diffraction pattern is shown in Figure 2b. Initial molecular replacement trials were performed in BALBES [32] using REFMAC5 [34] and a potential solution was found using the coordinates of PdxK from sheep brain ([33], PDB entry 1RFU,), which showed 14% sequence identity overall (Figs. 3a,b). There is a large insertion (104–309; 205 amino acids) in the *Pf*PdxK sequence that has no structural homologue. While the remaining 303 amino acids of *Pf*PdxK have a reasonable homology (28% identity) with 1rfu, we believe that this unmodelled portion may explain why the molecular-replacement solution and initial R factors are worse than might have been anticipated. However, the structure solution and refinement of *Pf*PdxK are in progress and will be reported elsewhere. The determined structure is likely to aid in dissecting the plasmodial vitamin B_6 metabolism and further anti-malarial drug design.

Figure 3

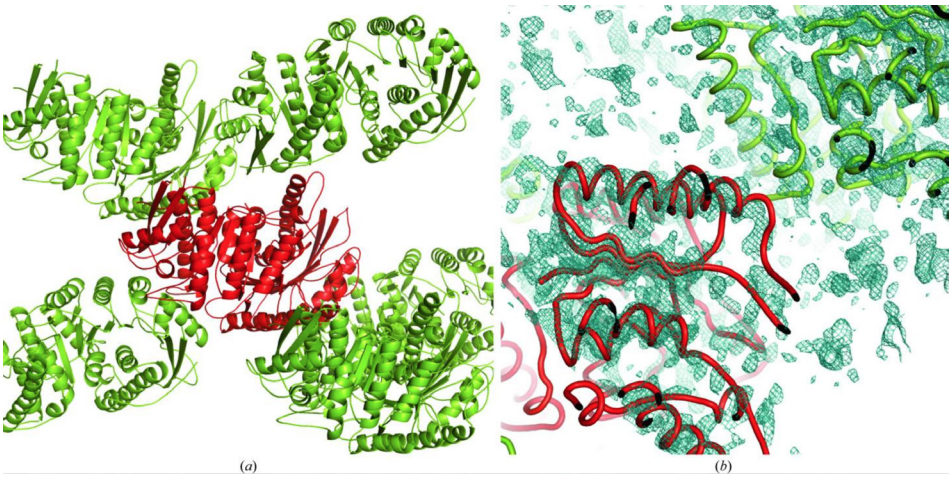

(a) A diagram showing the preliminary model of the *Pf*PdxK asymmetric unit. The molecular-replacement solution is shown in red and symmetry-related molecules are shown in green. (b) A diagram showing the preliminary $2F_o - F_c$ electron-density map contoured at 1.4σ. The map was calculated with weighted phases from REFMAC5 [34] following restrained refinement of the molecular-replacement solution. These diagrams were created using PyMOL (v.1.5.0.4; Schrödinger).

6. References

1. Guerin PJ, Olliaro P, Nosten F, Druilhe P, Laxminarayan R, Binka F, et al. Malaria: current status of control, diagnosis, treatment, and a proposed agenda for research and development. Lancet Infect Dis. 2002;2(9):564-73. PubMed PMID: 12206972.

2. WHO. World Malaria Report. World Health Organisation. 2013;(Geneva, Switzerland).

3. Olliaro P, Taylor WR, Rigal J. Controlling malaria: challenges and solutions. Trop Med Int Health. 2001;6(11):922-7. PubMed PMID: 11703847.

4. Bhattarai A, Ali AS, Kachur SP, Mårtensson A, Abbas AK, Khatib R, et al. Impact of artemisinin-based combination therapy and insecticide-treated nets on malaria burden in Zanzibar. PLoS Med. 2007;4(11):e309. doi: 10.1371/journal.pmed.0040309. PubMed PMID: 17988171; PubMed Central PMCID: PMCPMC2062481.

5. White NJ. The role of anti-malarial drugs in eliminating malaria. Malar J. 2008;7 Suppl 1:S8. doi: 10.1186/1475-2875-7-S1-S8. PubMed PMID: 19091042; PubMed Central PMCID: PMCPMC2604872.

6. Yang Y, Zhao G, Winkler ME. Identification of the pdxK gene that encodes pyridoxine (vitamin B6) kinase in Escherichia coli K-12. FEMS Microbiol Lett. 1996;141(1):89-95. PubMed PMID: 8764513.

7. Müller IB, Hyde JE, Wrenger C. Vitamin B metabolism in Plasmodium falciparum as a source of drug targets. Trends Parasitol. 2010;26(1):35-43. doi: 10.1016/j.pt.2009.10.006. PubMed PMID: 19939733.

8. Knöckel J, Müller IB, Butzloff S, Bergmann B, Walter RD, Wrenger C. The antioxidative effect of de novo generated vitamin B6

in Plasmodium falciparum validated by protein interference. Biochem J. 2012;443(2):397-405. doi: 10.1042/BJ20111542. PubMed PMID: 22242896.

9. Kronenberger T, Schettert I, Wrenger C. Targeting the vitamin biosynthesis pathways for the treatment of malaria. Future Med Chem. 2013;5(7):769-79. doi: 10.4155/fmc.13.43. PubMed PMID: 23651091.

10. Jain R, Jordanova R, Muller IB, Wrenger C, Groves MR. Purification, crystallization and preliminary X-ray analysis of the aspartate aminotransferase of Plasmodium falciparum. Acta Crystallogr Sect F Struct Biol Cryst Commun. 2010;66(Pt 4):409-12. PubMed PMID: 20383010.

11. Wrenger C, Muller IB, Schifferdecker AJ, Jain R, Jordanova R, Groves MR. Specific inhibition of the aspartate aminotransferase of Plasmodium falciparum. J Mol Biol. 2011;405(4):956-71. PubMed PMID: 21087616.

12. Wrenger C, Muller IB, Silber AM, Jordanova R, Lamzin VS, Groves MR. Aspartate aminotransferase: bridging carbohydrate and energy metabolism in Plasmodium falciparum. Curr Drug Metab. 2012;13(3):332-6. PubMed PMID: 22455555.

13. Wrenger C, Eschbach ML, Müller IB, Warnecke D, Walter RD. Analysis of the vitamin B6 biosynthesis pathway in the human malaria parasite Plasmodium falciparum. J Biol Chem. 2005;280(7):5242-8. doi: 10.1074/jbc.M412475200. PubMed PMID: 15590634.

14. Reeksting SB, Müller IB, Burger PB, Burgos ES, Salmon L, Louw AI, et al. Exploring inhibition of Pdx1, a component of the PLP synthase complex of the human malaria parasite Plasmodium falciparum. Biochem J. 2013;449(1):175-87. doi: 10.1042/BJ20120925. PubMed PMID: 23039077.

15. Müller IB, Bergmann B, Groves MR, Couto I, Amaral L, Beg-

ley TP, et al. The vitamin B1 metabolism of Staphylococcus aureus is controlled at enzymatic and transcriptional levels. PLoS One. 2009;4(11):e7656. doi: 10.1371/journal.pone.0007656. PubMed PMID: 19888457; PubMed Central PMCID: PMCPMC2766623.

16. Musayev FN, di Salvo ML, Ko TP, Gandhi AK, Goswami A, Schirch V, et al. Crystal Structure of human pyridoxal kinase: structural basis of M(+) and M(2+) activation. Protein Sci. 2007;16(10):2184-94. doi: 10.1110/ps.073022107. PubMed PMID: 17766369; PubMed Central PMCID: PMCPMC2204131.

17. Safo MK, Musayev FN, di Salvo ML, Hunt S, Claude JB, Schirch V. Crystal structure of pyridoxal kinase from the Escherichia coli pdxK gene: implications for the classification of pyridoxal kinases. J Bacteriol. 2006;188(12):4542-52. doi: 10.1128/JB.00122-06. PubMed PMID: 16740960; PubMed Central PMCID: PMCPMC1482971.

18. Park JH, Burns K, Kinsland C, Begley TP. Characterization of two kinases involved in thiamine pyrophosphate and pyridoxal phosphate biosynthesis in Bacillus subtilis: 4-amino-5-hydroxymethyl-2methylpyrimidine kinase and pyridoxal kinase. J Bacteriol. 2004;186(5):1571-3. PubMed PMID: 14973012; PubMed Central PMCID: PMCPMC344394.

19. Lum HK, Kwok F, Lo SC. Cloning and characterization of Arabidopsis thaliana pyridoxal kinase. Planta. 2002;215(5):870-9. doi: 10.1007/s00425-002-0799-0. PubMed PMID: 12244454.

20. Scott TC, Phillips MA. Characterization of Trypanosoma brucei pyridoxal kinase: purification, gene isolation and expression in Escherichia coli. Mol Biochem Parasitol. 1997;88(1-2):1-11. PubMed PMID: 9274862.

21. Jones DC, Alphey MS, Wyllie S, Fairlamb AH. Chemical, genetic and structural assessment of pyridoxal kinase as a drug target in the African trypanosome. Mol Microbiol. 2012;86(1):51-64. doi: 10.1111/j.1365-

2958.2012.08189.x. PubMed PMID: 22857512; PubMed Central PMCID: PMCPMC3470933.

22. Nettleship JE, Brown J, Groves MR, Geerlof A. Methods for protein characterization by mass spectrometry, thermal shift (ThermoFluor) assay, and multiangle or static light scattering. Methods Mol Biol. 2008;426:299-318. PubMed PMID: 18542872.

23. Ericsson UB, Hallberg BM, Detitta GT, Dekker N, Nordlund P. Thermofluor-based high-throughput stability optimization of proteins for structural studies. Anal Biochem. 2006;357(2):289-98. doi: 10.1016/j.ab.2006.07.027. PubMed PMID: 16962548.

24. Laemmli UK. Cleavage of structural proteins during the assembly of the head of bacteriophage T4. Nature. 1970;227(5259):680-5.

25. Mueller-Dieckmann J. The open-access high-throughput crystallization facility at EMBL Hamburg. Acta Crystallogr D Biol Crystallogr. 2006;62(Pt 12):1446-52. PubMed PMID: 17139079.

26. Bourenkov GP, Popov AN. A quantitative approach to data-collection strategies. Acta Crystallogr D Biol Crystallogr. 2006;62(Pt 1):58-64. PubMed PMID: 16369094.

27. Popov AN, Bourenkov GP. Choice of data-collection parameters based on statistic modelling. Acta Crystallogr D Biol Crystallogr. 2003;59(Pt 7):1145-53. PubMed PMID: 12832757.

28. Matthews BW. Solvent content of protein crystals. J Mol Biol. 1968;33(2):491-7. PubMed PMID: 5700707.

29. Kabsch W. XDS. Acta Crystallogr D Biol Crystallogr. 2010;66(Pt 2):125-32. doi: 10.1107/S0907444909047337. PubMed PMID: 20124692; PubMed Central PMCID: PMCPMC2815665.

30. Kabsch W. Integration, scaling, space-group assignment and post-refinement. Acta Crystallogr D Biol Crystallogr. 2010;66(Pt 2):133-44. doi: 10.1107/S0907444909047374. PubMed PMID: 20124693; PubMed Central PMCID: PMCPMC2815666.

31. Brünger AT. Free R value: a novel statistical quantity for assessing the accuracy of crystal structures. Nature. 1992;355(6359):472-5. PubMed PMID: 18481394.

32. Long F, Vagin AA, Young P, Murshudov GN. BALBES: a molecular-replacement pipeline. Acta Crystallogr D Biol Crystallogr. 2008;64(Pt 1):125-32. PubMed PMID: 18094476.

33. Li MH, Kwok F, Chang WR, Liu SQ, Lo SC, Zhang JP, et al. Conformational changes in the reaction of pyridoxal kinase. J Biol Chem. 2004;279(17):17459-65. doi: 10.1074/jbc.M312380200. PubMed PMID: 14722069.

34. Murshudov GN, Vagin AA, Dodson EJ. Refinement of macromolecular structures by the maximum-likelihood method. Acta Crystallogr D Biol Crystallogr. 1997;53(Pt 3):240-55. PubMed PMID: 15299926.